agronomy

MDPI

Article

Soil Fertility Enhancement by Organic Amendments in a Semiarid Calciustoll: Insights from Physicochemical, Enzymatic, and Microbial Responses

Zhicheng Bao [1,2], Chenglong Guan [1,2], Yingying Hao [1], Baoyu Chen [2], Jingkun Lu [2], Yunyun Sun [2], Jiuhui Chen [1,2], Yulong Yang [1,2], Chenyu Zhao [1], Hongjun Wang [2,*] and Biao Sui [1,*]

[1] College of Resources and Environment, Jilin Agricultural University, Changchun 130118, China; 20241837@mails.jlau.edu.cn (Z.B.); 15144441522@163.com (C.G.); hyy0920lh7@163.com (Y.H.); 15698259707@163.com (J.C.); a302545854@163.com (Y.Y.); chenyuzhao91@163.com (C.Z.)
[2] Institute of Agricultural Resources and Environment, Jilin Academy of Agricultural Sciences (Northeast Agricultural Research Center of China), Changchun 130033, China; bych76@jaas.com.cn (B.C.); lujingkun5258@163.com (J.L.); sunyunyun831212@163.com (Y.S.)
* Correspondence: whj603@126.com (H.W.); suibiao621@126.com (B.S.)

Abstract

Semiarid conditions, aeolian disturbance, and long-term cultivation have progressively weakened soil structure and nutrient-retention capacity in Calciustoll croplands of western Jilin Province. Although organic amendments improve soil quality, their comparative benefits after consecutive applications remain unclear. A two-year field experiment (2024–2025) compared four treatments: conventional compound fertilizer (CK), CK co-applied with cattle manure (CM) or granular organic fertilizer (GOF), and a biochar-based compound fertilizer (CBF) replacing CK. Soil physicochemical properties were assessed in both years, whereas enzyme activities and microbial communities were characterized in 2025. Fertility enhancement was evaluated using the soil quality index (SQI) and soil microbial index (SMI). All three amendments improved the Calciustoll to varying degrees. In the 0–20-cm layer, SQI peaked under CM in 2024 and CBF in 2025. SQI under CBF significantly exceeded that under CK by 76.96%, whereas SMI was significantly higher than that under every other treatment in both layers. CM promoted soil organic matter and nitrogen accumulation and increased C-related hydrolytic enzyme activities and urease activity, whereas CBF exhibited higher acid phosphatase activity. Exploratory pooled Spearman analyses suggested positive associations among SMI, SQI, and several enzyme activities; however, these relationships were not retained after accounting for treatment, soil depth, block, and plot-level pairing. Overall, CM more strongly promoted soil organic matter and nitrogen accumulation, whereas CBF produced broader SQI and SMI improvements after two years.

Keywords: Calciustoll; organic amendment; soil fertility; soil enzyme; microorganism

Check for updates

Academic Editor: Robert P. Larkin

Received: 28 September 2026
Revised: 4 November 2026
Accepted: 16 November 2026
Published: 18 November 2026

Copyright: © 2026 by the authors. Licensee MDPI, Basel, Switzerland. This article is an open access article distributed under the terms and conditions of the Creative Commons Attribution (CC BY) license.

1. Introduction

Drylands, including arid and semi-arid regions, cover approximately 45% of the global land area and are particularly vulnerable to land degradation and declining soil productivity [1]. Mollisols are among the world's important agricultural soils, and maintaining their soil organic carbon and structural stability under cultivation is important for their sustainable use [2]. Western Jilin Province, China, is semiarid with low and seasonally uneven precipitation. Farmland soil is frequently affected by wind erosion and water loss. Long-term cultivation in the region has also resulted in topsoil compaction, reduced aggregate

stability, organic matter loss, and a decline in nutrient-retention capacity. This constrains the maintenance and improvement of Calciustoll fertility [3]. Maize straw mulching and return can help mitigate wind erosion and water limitations by increasing surface cover, reducing wind erosion and evaporation, and supplying organic matter to the soil [4–6]. By loosening planting strips while minimizing overall soil disturbance, strip tillage can alleviate surface soil compaction [7,8]. Therefore, combining maize straw mulching and return with strip tillage supports soil and water conservation and improves conditions in the cultivated soil layer of Calciustolls [9]. However, tillage and straw return alone may provide only limited gains in soil organic matter accumulation and nutrient-retention capacity. Further improvements in soil structure and fertility remain key challenges for long-term agricultural production in the region.

Organic amendments can help address this challenge by supplying organic carbon and nutrients to soil and promoting aggregate formation under conservation tillage [10]. Organic amendments can increase inputs of soil organic matter and nutrients. However, substantial differences in their composition and physical form may lead to different fertility outcomes. Rich in organic matter and nitrogen, cattle manure can directly add organic carbon and nutrients to soil after application [11,12]. Granular organic fertilizers provide relatively concentrated nutrients in a processed form that is convenient to apply [13], whereas biochar-based compound fertilizers couple organic carbon input with controlled-release characteristics [14–17]. Beyond nutrient supply, the use of manure and biochar-based fertilizers has also attracted attention in sustainable agriculture and climate-change mitigation because of their potential contributions to nutrient recycling and soil carbon management [7,12]. Accordingly, different amendments may influence soil quality through distinct combinations of organic matter inputs, nutrient supply, and structural improvement. However, research on fertility enhancement by organic amendments has largely focused on the black soil region of northeastern China, and evidence for Calciustolls in semiarid western Jilin remains limited. The region is subject to multiple constraints, including aeolian disturbance, water limitation, and soil structural degradation, yet the field-scale fertility improvement achieved by different organic amendments under local agricultural conditions remains insufficiently understood. In particular, under strip tillage with maize straw mulch retention, it is still unclear whether cattle manure, granular organic fertilizer, and biochar-based compound fertilizer differ in their effects on soil structure, nutrient status, and overall soil fertility.

Improvement in soil quality encompasses not only greater organic matter and nutrient contents, but also changes in soil structure, biochemical processes, and microbial characteristics. The activities of soil enzymes involved in carbon, nitrogen, and phosphorus transformations can indicate the status of soil nutrient cycling [18,19]. Bacterial and fungal communities respond to organic amendment inputs and changes in the soil environment, and shifts in their composition can provide biological evidence of altered soil conditions [20–22]. Because no single indicator can comprehensively capture fertility improvement, soil physicochemical and microbial indicators must be integrated [23]. The soil quality index (SQI) [24] and soil microbial index (SMI) provide integrated measures of soil quality and microbial characteristics. These can facilitate comparisons of fertility improvement among organic amendments.

Against this background, we conducted a two-year field experiment (2024–2025) to compare how cattle manure, granular organic fertilizer, and biochar-based compound fertilizer affected the fertility of a Calciustoll managed with strip tillage and maize straw mulching and return. The contribution of this study lies in the field-based comparison of physicochemical, enzymatic, and microbial responses to three amendment treatments under semiarid Calciustoll conditions over two consecutive years. The experiment ad-

dressed three questions: (1) Do organic amendments differ in their effects on soil structure, nutrients, and overall fertility, and do these differences vary between years? (2) In addition to improving soil physicochemical properties, do the amendments affect C_hydro, UE, and ACP activities and bacterial and fungal communities, and are physicochemical properties associated with microbial changes? (3) Do SQI, SMI, and C_hydro, UE, and ACP activities show coordinated variation, and do the amendments produce different integrated fertility responses? Given their differences in composition and nutrient contents, we hypothesized that although all three amendments would improve the Calciustoll to some extent, they would differ in their effects on soil structure, nutrients, enzyme activities, microbial communities, and consequently overall fertility. We further hypothesized that SQI, SMI, C_hydro, UE, and ACP activities would covary and jointly reflect fertility improvement under the different amendments.

2. Materials and Methods

2.1. Study Site

A field experiment was conducted during 2024–2025 in Xieli Village, Wohu Town, Shuangliao City, Siping, Jilin Province, China (43.38° N, 123.35° E). Located in semiarid western Jilin on the southern Songnen Plain, the site has a temperate continental monsoon climate. The mean annual temperature and precipitation are 6.9 °C and 494 mm, respectively. The frost-free period is approximately 153 d, and the annual sunshine duration is 2820.6 h. Under the Chinese Soil Genetic Classification, the experimental soil is a light Calcic Chernozem, corresponding to a Calciustoll under the United States Department of Agriculture (USDA) Soil Taxonomy. Before the experiment, the entire field had been managed by local farmers under the same conventional maize production practices. Therefore, three soil samples were randomly collected across the field, and the mean values of the three samples were used to represent the initial soil properties of the experimental site. At the beginning of the experiment, soil organic matter (SOM), total nitrogen (TN), and available potassium (AK) were 19.77 g kg^{-1}, 0.42 g kg^{-1}, and 160.77 mg kg^{-1}, respectively. Available phosphorus (AP), available nitrogen (AN), and bulk density (BD) were 10.64 mg kg^{-1}, 100.18 mg kg^{-1}, and 1.42 g cm^{-3}, respectively.

2.2. Experimental Design

The same strip-tillage and maize straw return regime was applied to each treatment. The experiment followed a randomized complete block design with three blocks, each containing one plot per treatment, with treatments randomly assigned within each block. The maize cultivar Liangyu 99 was planted in a wide–narrow row pattern, with alternating row spacings of 80 and 40 cm, at a final plant population density of 73,000 plants ha^{-1}. The conventional compound fertilizer control (CK) received 1000 kg ha^{-1} of conventional compound fertilizer (N–P_2O_5–K_2O = 26–10–12) and no organic amendment. The cattle manure co-application treatment (CM) combined the same fertilizer dose with 20 m^3 ha^{-1} of cattle manure. The granular organic fertilizer co-application treatment (GOF) received the same conventional compound fertilizer dose as CK plus 100 kg ha^{-1} of granular organic fertilizer. In the biochar-based compound fertilizer replacement treatment (CBF), 1000 kg ha^{-1} of biochar-based compound fertilizer (N–P_2O_5–K_2O = 26–10–12) completely replaced the conventional compound fertilizer. The experiment included three blocks, with each treatment randomly assigned to one plot within each block, resulting in 12 plots and three replicates per treatment with each covering 400 m^2. The treatment assigned to each plot remained unchanged between 2024 and 2025, and the corresponding fertilizers and organic amendments were applied in both years. Cattle manure, decomposed for approximately two years and obtained from local farmers, was applied at 20 m^3 ha^{-1} (equivalent to

17 t ha^{-1} fresh weight at a wet bulk density of 0.85 t m^{-3}). Its moisture content was 31% (69% dry matter; 11.73 t ha^{-1} dry matter), and it contained 11.83% C, 0.34% N, 0.67% P_2O_5, and 0.81% K_2O on a fresh-weight basis. The granular organic fertilizer had a moisture content of 3.0%. On a dry-weight basis, it contained 27.4% organic carbon, 7.3% N, 0.7% P_2O_5, and 1.4% K_2O. The biochar-based compound fertilizer contained 8% carbon and consisted of fertilizer granules with a carbon coating and controlled release characteristics. The application rates followed local farmer practices. The annual C, N, P_2O_5, and K_2O inputs under each treatment are presented in Supplementary Table S1. All other field management practices were identical across treatments. Because carbon, organic matter, and total nutrient inputs differed among the three amendment treatments, this study compared their overall effects under actual field management regimes. Grain yield was determined at maturity in both 2024 and 2025. Two representative 10-m rows were harvested from each plot, and grain moisture content was measured. Grain yield was standardized to 14% moisture content.

2.3. Soil Physicochemical Properties and Soil Quality Index

At maize harvest in each year, soil samples were collected from three sampling points across maize planting rows and inter-row spaces in each plot at depths of 0–20 and 20–40 cm. Samples from the three points at each depth were pooled separately to obtain one composite sample per plot and depth. A portion of each fresh sample was kept at low temperature for enzyme activity and microbial analyses, and the remainder was air dried for physicochemical measurements. Physicochemical properties were determined in samples from both 2024 and 2025, whereas enzyme activities and microbial communities were analyzed only in the 2025 samples. The same set of 24 samples was used for bacterial and fungal sequencing.

Measurements included BD, total soil porosity (TSP), >0.25 mm water-stable aggregates (WSA), SOM, TN, AN, AP, and AK. BD was measured using the core method, and TSP was calculated using Equation (1). A particle density of 2.65 g cm^{-3} was assumed as a conventional value for mineral soils. Because particle density was not directly measured, TSP represents an estimated value calculated from BD. WSA was determined using the Yoder wet-sieving method [25]. SOM was measured using potassium dichromate oxidation with external heating, TN using the Kjeldahl method, AN using alkaline hydrolysis diffusion, AP using sodium bicarbonate extraction followed by molybdenum–antimony colorimetry, and AK using flame photometry.

$$TSP = (1 - BD/2.65) \times 100\% \quad (1)$$

Seven indicators, including SOM, TN, AN, AP, AK, WSA, and BD, from all 48 samples collected in 2024–2025, were equally weighted in the SQI calculation. The positive indicators of SOM, TN, AN, AP, AK, and WSA were standardized using Equation (2), while the negative indicator BD was reverse-standardized using Equation (3). For each indicator, x_min and x_max denote the minimum and maximum values across all 48 samples from both years, respectively. For each sample, SQI was calculated as the arithmetic mean of the seven standardized scores [24]. Applying a common standardization range to 2024 and 2025 allowed for the comparison of relative soil quality differences among treatments and between years. Equal weighting was used for transparent relative comparisons, and the resulting min–max scores were considered dataset-specific rather than absolute soil quality thresholds. Derived from BD, TSP was omitted from SQI to prevent duplication of information.

$$S_i = (x_i - x_{min})/(x_{max} - x_{min}) \quad (2)$$

$$S_i = (x_{max} - x_i)/(x_{max} - x_{min}) \quad (3)$$

2.4. Soil Enzyme Activities and Related Enzyme-Activity Ratios

In 2025, six soil enzyme activities, including α-glucosidase (α-GC), β-glucosidase (β-GC), cellobiohydrolase (CBH), xylanase (Xyl), urease (UE), and acid phosphatase (ACP), were determined using colorimetric assay kits from the same manufacturer (Suzhou Grace Biotechnology Co., Ltd., Suzhou, China). All assays were performed using 0.3 g of dry soil following the corresponding kit protocols. Xyl activity was determined by the 3,5-dinitrosalicylic acid (DNS) colorimetric method after incubation at 40 °C for 6 h, with absorbance measured at 540 nm. CBH activity was determined using a reducing-sugar colorimetric assay with a reaction time of 1 h. α-GC and β-GC activities were determined using p-nitrophenol (PNP)-based colorimetric assays with reaction times of 1 h, whereas ACP activity was determined using a PNP-based assay with a reaction time of 24 h. UE activity was determined colorimetrically by measuring the NH_3-N released during urea hydrolysis after a 24-h reaction.

Enzyme activities were calculated using the assay-specific equations recorded in the original worksheets and expressed on a dry-soil mass basis. The original daily activities of α-GC, β-GC, and ACP were converted to hourly rates by dividing by 24. CBH and Xyl activities were converted to molar assay equivalents using the conversion factors applied in the original calculations (180.16 and 150.13, respectively), with Xyl additionally converted from mg to μg and from daily to hourly activity. UE activity was converted from μg NH_3-N g^{-1} d^{-1} to μmol N g^{-1} h^{-1} using the molar mass of N (14.007 g mol^{-1}) and a 24-h conversion. C_hydro was calculated as the sum of Xyl, CBH, α-GC, and β-GC activities. C_hydro:ACP, C_hydro:UE, and UE:ACP were calculated as relative enzyme activity ratios, and SLCR was calculated according to Equation (4). Because the C-related enzymes were measured using different substrates and analytical endpoints, C_hydro was treated as an operational composite of enzyme activities rather than a direct measure of soil carbon mineralization.

$$\text{SLCR} = (\text{CBH} + \text{Xyl})/(\text{α-GC} + \text{β-GC}) \quad (4)$$

2.5. Soil Microbial Sequencing and Community Analysis

Amplicon sequencing of bacterial 16S rRNA genes and fungal internal transcribed spacer (ITS) regions was performed on the 24 soil samples collected in 2025. Total DNA was extracted using a MagBeads FastDNA Kit for Soil (MP Biomedicals, LLC, Irvine, CA, USA; Cat. No. 116564384). Primers 338F/806R amplified the bacterial V3–V4 region, and primers ITS5/ITS2 amplified the fungal ITS1 region. Following purification and quantification, amplicons underwent 2 × 250 bp paired-end sequencing on an Illumina NovaSeq 6000 platform(Illumina, Inc., San Diego, CA, USA). QIIME2 2024.5 was used for primer removal, quality filtering, denoising, read merging, and chimera removal. Subsequently, DADA2 generated amplicon sequence variant (ASV) tables [26,27]. Taxonomic assignments were made using SILVA release 138 for bacteria and UNITE release 9.0 for fungi [28,29].

All samples were rarefied to 95% of the lowest valid sequence count before Chao1 and Shannon indices were calculated. Treatment differences in α-diversity within each soil layer were evaluated using the Kruskal–Wallis test. Principal coordinate analysis (PCoA) was based on Bray–Curtis distances calculated from the relative sample abundance. The effects of treatment, soil depth, and their interactions on bacterial and fungal community composition were tested using permutational multivariate analysis of variance (PERMANOVA) with 9999 permutations [30]. Permutations were restricted according to the block and paired-plot structure, and multivariate dispersion was assessed using PERMDISP. Redundancy analysis (RDA) and Mantel tests were performed at the genus level. Community data were Hellinger-transformed before RDA [31], and environmental variables were standardized and screened using variance inflation factors. The significance of the RDA model and

environmental variables was tested using 999 permutations. Mantel tests used Bray–Curtis dissimilarities for community data, Euclidean distances for environmental variables, and 999 permutations. For both marginal RDA and Mantel tests, significance was defined as $p < 0.05$.

2.6. Cross-Kingdom Co-Occurrence Network, Cohesion, and Soil Microbial Index

Bacterial and fungal ASV abundance data from the 24 soil samples collected in 2025 were used to construct a cross-kingdom co-occurrence network [32,33]. ASVs were retained when their pooled relative abundance across the 24 samples exceeded 0.1%, calculated separately for each kingdom. The original network included bacterial–fungal associations with $|\rho| \geq 0.60$ and $p < 0.01$. To account for multiple testing, Benjamini–Hochberg (BH) correction was applied to all 23,532 candidate bacterial–fungal pairs. Associations with $q < 0.05$ and $|\rho| \geq 0.60$ were used to construct an FDR-filtered network for sensitivity analysis. Network topology was quantified using igraph, and degree, betweenness, and PageRank were used to evaluate node centrality. Network-central taxa were defined as ASVs for which at least two of the three metrics fell within the top 10% of all nodes [34]. The enrichment of fungi among these taxa was evaluated using a one-sided Fisher's exact test and a null-model test with 10,000 random rewirings that preserved the bipartite structure and node-degree sequence [35].

Network robustness was evaluated based on changes in the size of the largest connected component. The corresponding areas under the curve were compared between random node removal based on 1000 simulations and targeted removal in descending order of initial betweenness centrality. The effect of removing network-central taxa on network connectivity was tested against 10,000 random removals of the same number of nodes.

Positive and negative cohesion of bacteria and fungi were calculated separately. ASVs with a mean relative abundance $< 0.01\%$ or prevalence $< 20\%$ were first removed, after which correlations were estimated using SparCC [36]. p values were derived from 100 permutations, and associations were retained when $|r| > 0.30$ and $p < 0.05$. Sample-level cohesion was calculated according to Herren and McMahon [37].

The SMI was derived from the 24 soil samples collected in 2025. Following the general concept of integrating multiple microbial attributes into a composite index [37], five study-specific indicators were selected: bacterial and fungal Shannon indices, bacterial and fungal positive cohesion, and the summed relative abundance of the 18 network-central taxa identified in the original cross-kingdom network. These indicators represented α-diversity, sample-level community cohesion [36], and the abundance of taxa occupying central network positions [38], respectively. All five indicators were Z-score standardized, and PCA was performed on these same 24 samples. Weights were calculated from the absolute PC1 loadings (Equation (5)), reflecting loading magnitude rather than direction. Bacterial positive cohesion had a negative PC1 loading (−0.214), whereas the other four indicators had positive loadings. Therefore, the absolute-loading weighted sum (Equation (6)) was not equivalent to the signed PC1 score. The raw composite value was subsequently standardized as a Z-score to obtain the final SMI. Alternative weighting schemes and indicator combinations were evaluated to assess the consistency of treatment rankings (Table S3). The SMI was treated as a study-specific exploratory index rather than a validated measure of microbial functioning or soil health.

$$w_k = |l_k| / \Sigma_j |l_j| \quad (5)$$

$$SMI_{raw} = \Sigma(w_k \, Z_k) \quad (6)$$

2.7. Data Analysis and Statistical Methods

Soil physicochemical properties were analyzed using linear mixed-effects models with treatment, year, depth, and their interactions as fixed effects. Block was included as a fixed blocking factor, and plot identity was specified as a random intercept. Response-specific residual variance structures were selected based on model fit. Fixed effects were tested using marginal F-tests, with Tukey-adjusted comparisons within each year × depth combination [38]. The same testing procedure was used to compare soil enzyme activities among treatments within each Enzyme × Depth combination. Within each soil layer, SMI and positive and negative cohesion were analyzed separately using one-way ANOVA, followed by Tukey's honestly significant difference test. Exploratory associations among SMI, SQI, and soil enzyme activities were initially examined using Spearman's rank correlation. To account for experimental grouping and repeated observations, rank-transformed mixed-effects models were fitted with Treatment × Depth and Block as fixed effects and PlotID as a random intercept. p values from 26 unique association tests were adjusted using the Benjamini–Hochberg procedure. Within-depth analyses and plot-paired permutation tests were conducted as sensitivity analyses. ANOVA and post hoc comparisons were performed using SPSS version 24.0, and all other data processing and statistical analyses were performed using R version 4.5.0.

3. Results

3.1. Effects of Different Organic Amendments on the Physicochemical Properties and Soil Quality Index of the Calciustoll

Treatment responses varied with year and soil depth (Table 1). In 2024, CM showed higher surface SOM and TN than CK. In 2025, CBF exhibited lower surface BD and higher WSA and available nutrient contents (AN, AP, and AK) than CK. However, these responses were not consistent in the 20–40 cm layer. In the 0–20 cm layer in 2024, CM, GOF, and CBF reduced BD significantly by 7.64%, 6.25%, and 8.33%, respectively, compared with CK. CM produced the largest increases in SOM, TN, and AN, at 18.47%, 25.58%, and 19.94%, respectively. Under CBF, AK reached the highest mean value of 215.25 mg kg^{-1}, representing a numerical increase of 25.99% compared with CK, although the difference was not significant. The three organic amendment treatments did not exhibit significant differences in WSA (>0.25 mm). The improvements in surface soil properties under each amendment were more pronounced in 2025. Relative to CK, BD declined significantly by 7.91%, 7.91%, and 9.35% under CM, GOF, and CBF, respectively. CM showed the highest mean SOM content, which was 19.76% higher than that under CK. The highest AN, AP, and AK were observed under CBF, representing significant increases of 37.09%, 64.74%, and 24.87%, respectively. WSA increased significantly under CBF and CM by 18.80% and 17.05%, respectively. In 2024, CBF resulted in the highest AN and AK values but the lowest WSA. In 2025, CBF showed the highest mean values of AN, AP, AK, and WSA in the 0–20 cm layer. In both years, CM maintained relatively high SOM and TN levels in the 0–20 cm layer. The Treatment × Year × Depth interaction significantly affected BD, AP, AK, and WSA (Table 1).

SQI distinguished soil quality responses among treatments (Figure 1). Compared with CK in the 0–20 cm layer, CM and CBF increased SQI significantly by 54.31% and 39.87%, respectively, in 2024. In the same 0–20 cm layer in 2025, significant increases of 61.10%, 49.41%, and 76.96% were observed under CM, GOF, and CBF, respectively. Thus, the treatment that produced the highest SQI shifted from CM in 2024 to CBF in 2025. At 20–40 cm, CM significantly increased SQI compared with CK in 2024, whereas GOF and CBF did not differ significantly between CK and CM. Although CBF produced the highest SQI in 2025, no significant treatment differences were detected.

Table 1. Physicochemical properties of the Calciustoll under different organic amendment treatments during 2024–2025 and results of linear mixed-effects models (mean ± standard error (SE), $n = 3$).

Year	Depth (cm)	Treatment	BD (g cm^{-3})	TSP (%)	WSA > 0.25 mm (%)	SOM (g kg^{-1})	TN (g kg^{-1})	AN (mg kg^{-1})	AP (mg kg^{-1})	AK (mg kg^{-1})
2024	0–20	CK	1.4367 ± 0.0120 a	45.79 ± 0.45 a	26.94 ± 2.65 a	20.90 ± 1.04 b	0.433 ± 0.003 c	156.45 ± 12.62 a	21.89 ± 0.20 c	170.85 ± 7.18 a
2024	0–20	CM	1.3267 ± 0.0033 b	49.94 ± 0.13 b	38.04 ± 5.37 a	24.76 ± 0.41 a	0.543 ± 0.018 a	187.64 ± 13.20 a	27.51 ± 0.44 a	172.10 ± 12.33 a
2024	0–20	GOF	1.3467 ± 0.0145 b	49.18 ± 0.55 b	30.57 ± 6.15 a	22.77 ± 0.15 ab	0.467 ± 0.028 bc	157.28 ± 14.02 a	22.66 ± 0.14 bc	197.15 ± 8.95 a
2024	0–20	CBF	1.3233 ± 0.0033 b	50.06 ± 0.13 b	28.93 ± 1.60 a	23.24 ± 0.95 ab	0.533 ± 0.003 ab	173.63 ± 13.67 a	23.33 ± 0.47 b	215.25 ± 14.15 a
2024	20–40	CK	1.6533 ± 0.0120 a	37.61 ± 0.45 a	37.16 ± 0.36 a	20.73 ± 1.10 a	0.273 ± 0.003 b	109.78 ± 1.07 c	17.42 ± 0.05 a	134.05 ± 6.32 b
2024	20–40	CM	1.6500 ± 0.0058 a	37.74 ± 0.22 a	35.47 ± 0.99 a	23.43 ± 0.59 a	0.427 ± 0.022 a	135.48 ± 5.05 ab	16.80 ± 0.22 a	125.70 ± 7.66 b
2024	20–40	GOF	1.6233 ± 0.0186 a	38.74 ± 0.70 a	28.22 ± 0.20 b	21.76 ± 0.93 a	0.323 ± 0.012 b	125.35 ± 1.23 bc	16.70 ± 0.20 a	158.00 ± 6.70 a
2024	20–40	CBF	1.6800 ± 0.0115 a	36.60 ± 0.44 a	20.27 ± 2.01 c	22.06 ± 0.36 a	0.347 ± 0.009 ab	148.25 ± 8.03 a	17.05 ± 0.21 a	171.65 ± 1.77 a
2025	0–20	CK	1.3908 ± 0.0011 a	47.52 ± 0.04 a	42.23 ± 0.72 b	21.31 ± 2.33 a	0.442 ± 0.004 a	121.33 ± 5.38 b	15.60 ± 0.35 b	153.30 ± 2.75 b
2025	0–20	CM	1.2819 ± 0.0010 b	51.63 ± 0.04 b	49.43 ± 0.08 a	25.52 ± 1.09 a	0.518 ± 0.021 a	152.97 ± 3.93 a	23.37 ± 1.95 a	162.33 ± 16.35 ab
2025	0–20	GOF	1.2810 ± 0.0011 b	51.66 ± 0.04 b	39.12 ± 0.08 c	23.65 ± 1.09 a	0.490 ± 0.016 a	149.93 ± 0.84 a	23.23 ± 1.04 a	188.00 ± 1.83 ab
2025	0–20	CBF	1.2588 ± 0.0003 c	52.50 ± 0.01 c	50.17 ± 0.24 a	24.91 ± 1.79 a	0.506 ± 0.016 a	166.33 ± 5.80 a	25.70 ± 0.25 a	191.43 ± 1.68 a
2025	20–40	CK	1.5115 ± 0.0309 b	42.96 ± 1.17 b	37.51 ± 0.34 d	20.51 ± 1.15 a	0.236 ± 0.003 a	119.00 ± 11.11 a	15.67 ± 1.02 a	147.60 ± 0.67 a
2025	20–40	CM	1.6515 ± 0.0115 a	37.68 ± 0.43 a	41.69 ± 0.11 b	23.26 ± 0.71 a	0.360 ± 0.010 a	128.57 ± 14.24 a	17.83 ± 2.89 a	168.37 ± 2.06 a
2025	20–40	GOF	1.6422 ± 0.0045 a	38.03 ± 0.17 a	40.15 ± 0.01 c	21.89 ± 0.92 a	0.355 ± 0.091 a	128.50 ± 3.31 a	15.53 ± 0.72 a	132.80 ± 10.68 a
2025	20–40	CBF	1.5810 ± 0.0041 ab	40.34 ± 0.16 ab	51.92 ± 0.12 a	22.28 ± 0.53 a	0.393 ± 0.063 a	137.10 ± 3.86 a	14.07 ± 0.13 a	159.50 ± 8.56 a
Treatment			*	*	*	*	*	*	*	*
Year			***	***	***	ns	ns	*	* *	ns
Depth			***	***	ns	*	***	***	***	***
Treatment × Year			***	***	***	ns	ns	ns	*	**
Treatment × Depth			***	***	ns	ns	ns	ns	***	*
Year × Depth			ns	ns	ns	ns	ns	*	ns	**
Treatment × Year × Depth			***	***	**	ns	ns	ns	**	**

Within a given Year × Depth combination, different lowercase letters denote significant treatment differences based on Tukey-adjusted pairwise comparisons from the linear mixed-effects model ($p < 0.05$). Fixed-effect tests for Treatment, Year, Depth, and their interactions from the linear mixed-effects model are presented at the bottom of the table.Asterisks indicate significance levels: $p < 0.05$ (*), $p < 0.01$ (**), and $p < 0.001$ (***); ns indicates no significant effect ($p \geq 0.05$).

3.2. Effects of Different Organic Amendments on Soil Enzyme Activities and Their Ratios

Soil enzyme activities differed significantly among organic amendment treatments in 2025 (Figure 2A). In the 0–20 cm layer, CM produced the highest activities of α-GC, β-GC, CBH, Xyl, and UE, which significantly exceeded those under CK by 63.9%, 48.7%, 52.6%, 89.0%, and 70.3%, respectively. At 20–40 cm, CM produced the highest α-GC, β-GC, Xyl, and UE activities, with significant increases of 134.5%, 77.2%, 103.6%, and 136.4%, respectively, over CK. In contrast, CBF significantly increased ACP activity compared with CK in both layers, by 48.5% at 0–20 cm and 45.1% at 20–40 cm.

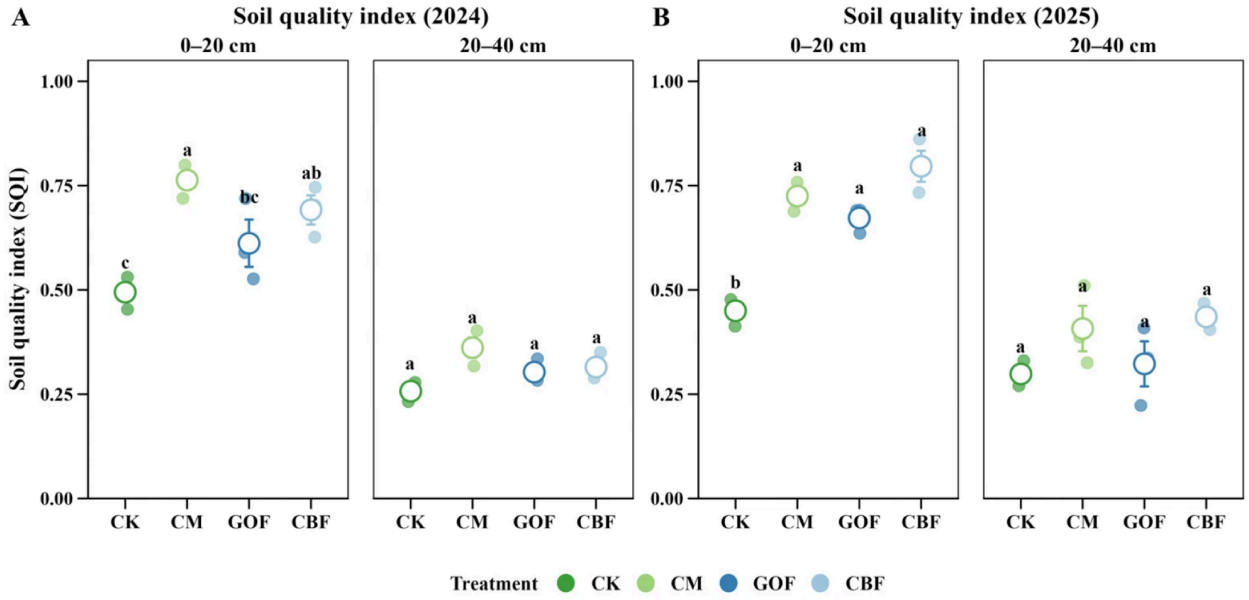


Figure 1. Soil quality index (SQI) under different fertilization treatments in 2024 and 2025. Panels (**A**,**B**) show SQI in the 0–20 and 20–40 cm soil layers in 2024 and 2025, respectively. Small colored points represent field replicates, and open symbols with error bars represent mean ± SE. Different lowercase letters indicate significant differences among treatments within the same year and soil layer based on Tukey-adjusted pairwise comparisons from the linear mixed-effects model ($p < 0.05$). CK, conventional compound fertilizer; CM, cattle manure co-application; GOF, granular organic fertilizer co-application; CBF, biochar-based compound fertilizer substitution.

Treatment effects on enzyme activity ratios were stronger in the 20–40 cm layer (Figure 2B). Compared with CK, CM, GOF, and CBF lowered C_hydro:UE by 48.6%, 47.2%, and 34.0%, respectively, as well as SLCR by 41.3%, 41.3%, and 36.8%, respectively. Conversely, UE:ACP increased by 88.4%, 58.8%, and 17.8%, respectively. C_hydro:ACP was lower under GOF and CBF than under CK but changed little under CM.

3.3. Effects of Different Organic Amendments on Soil Microbial Community Characteristics and the Soil Microbial Index

3.3.1. Microbial α-Diversity and Community Composition

Treatment effects were not significant for most microbial α-diversity indices (Figure 3A–D). Neither fungal Chao1 nor fungal Shannon differed significantly among treatments in either soil layer. Moreover, bacterial Chao1 and Shannon showed no significant treatment differences at 0–20 cm. At 20–40 cm, both bacterial indices differed significantly among treatments ($p = 0.025$), with the values generally being the highest under CBF and the lowest under CK, with CM and GOF occupying intermediate positions.

Bacterial community composition was separated by treatment and soil layer in PCoA (Figure 3E). Treatments occupied different positions in the ordination space, and CBF demonstrated a relatively clear separation from the other treatments. PCoA1 accounted for 28.3% of the community variation, and PCoA2 accounted for 15.3%. In addition, PERMANOVA detected significant effects of Treatment, Depth, and Treatment × Depth on bacterial community composition. Treatment, Depth, and Treatment × Depth explained 32.1% ($R^2 = 0.321$, $p < 0.001$), 15.0% ($R^2 = 0.150$, $p < 0.001$), and 14.1% ($R^2 = 0.141$, $p = 0.005$), respectively.

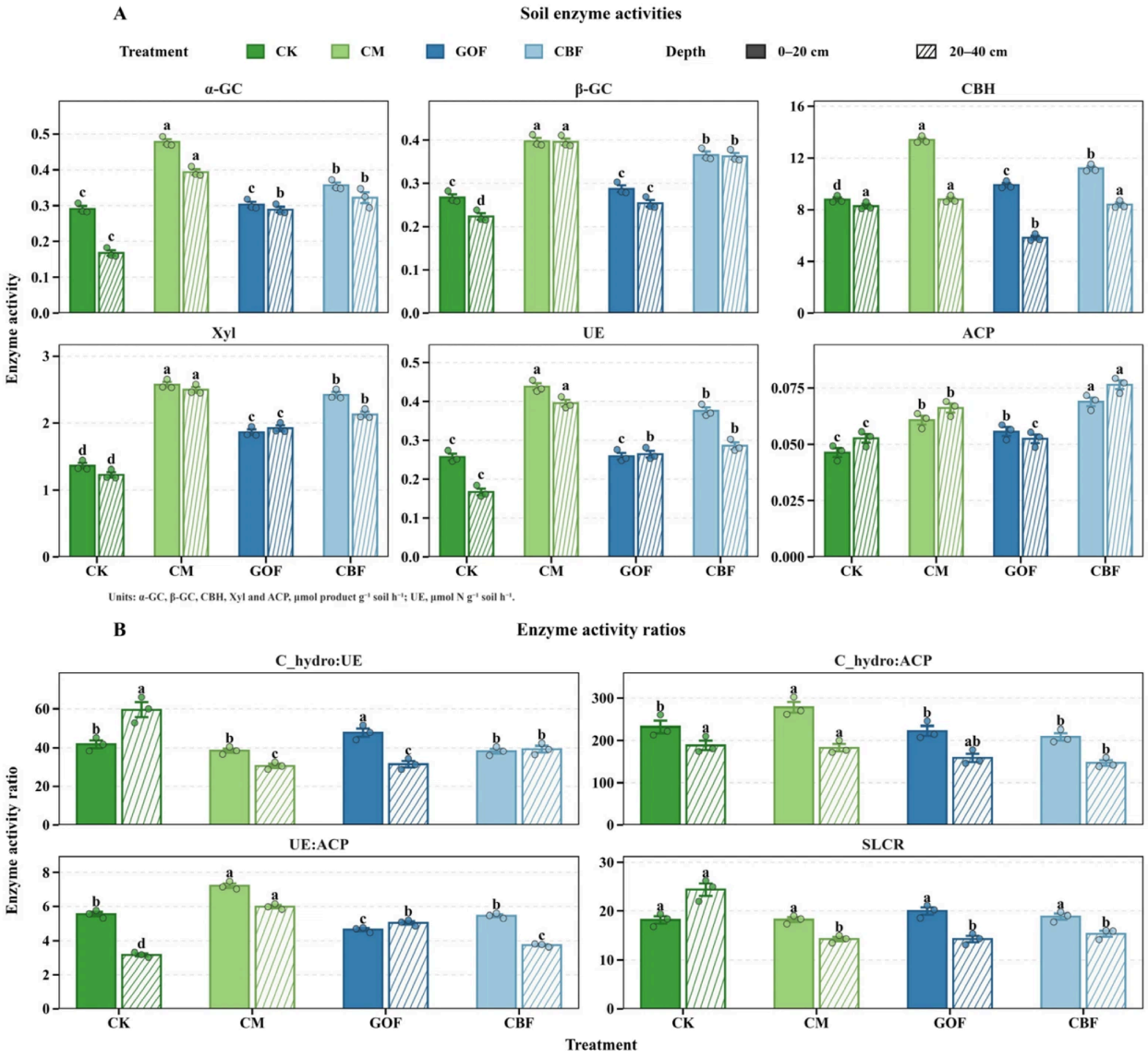


Figure 2. Soil enzyme activities and enzyme activity ratios under different fertilization treatments in 2025. (**A**) Activities of α-GC, β-GC, CBH, Xyl, UE, and ACP in the 0–20 cm and 20–40 cm soil layers; bars and error bars represent mean ± SE, and small points represent the three field replicates. Colors indicate treatments, and solid and hatched bars indicate the 0–20 cm and 20–40 cm soil layers, respectively. Units for α-GC, β-GC, CBH, Xyl, and ACP are μmol product g^{-1} soil h^{-1}, and the unit for UE is μmol N g^{-1} soil h^{-1}. Different lowercase letters within the same enzyme and soil layer indicate significant treatment differences based on Tukey-adjusted pairwise comparisons ($p < 0.05$). (**B**) C_hydro:UE, C_hydro:ACP, UE:ACP, and SLCR calculated from soil enzyme activities; C_hydro represents the summed activities of α-GC, β-GC, CBH, and Xyl, and SLCR represents (CBH + Xyl)/(α-GC + β-GC). Bars, error bars, raw replicates, and significance letters are defined as in (**A**).

The fungal community composition was similarly separated among treatments and soil layers (Figure 3F), with PCoA1 and PCoA2 accounting for 12.6% and 10.1% of the variation, respectively. Significant PERMANOVA effects were detected for Treatment, Depth, and Treatment × Depth; these factors explained 26.3%, 6.5%, and 17.3% of the fungal community variation, respectively (all $p < 0.001$).

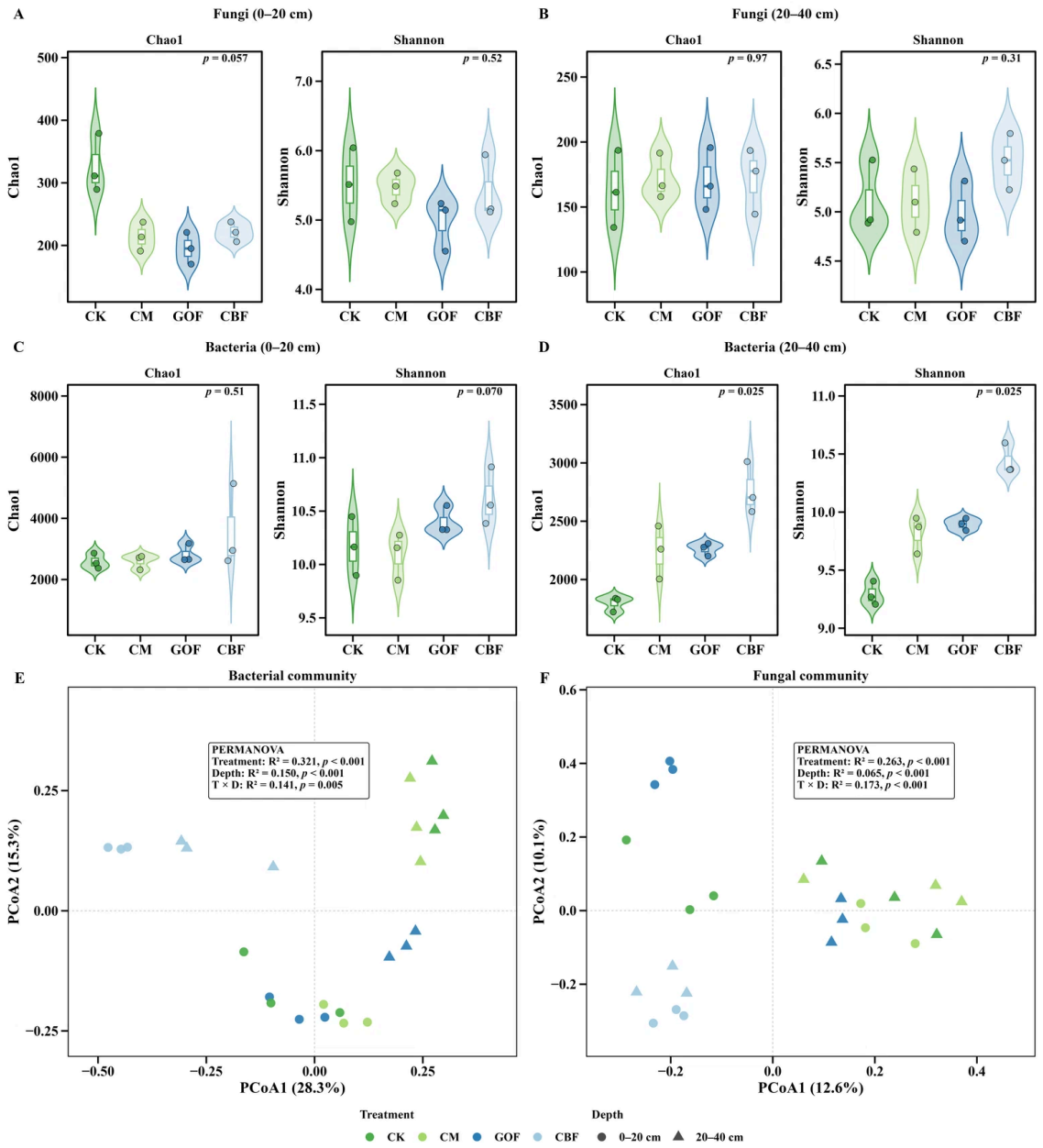


Figure 3. Bacterial and fungal α-diversity and community composition under different fertilization treatments. Panels (**A**,**B**) show fungal Chao1 and Shannon indices, respectively, for the 0–20 and 20–40 cm soil layers; panels (**C**,**D**) show the corresponding bacterial indices. Panels (**E**,**F**) show PCoA of bacterial and fungal communities based on Bray–Curtis dissimilarities, respectively. Colors indicate treatments, shapes indicate soil layers, and inset boxes show PERMANOVA results.

3.3.2. Relationships Between Soil Environmental Factors and Microbial Community Composition

RDA identified significant associations between soil environmental factors and both bacterial and fungal community composition (Figure 4A,C). For bacteria, RDA1 and RDA2 explained 31.50% and 11.87% of the community variation, respectively, and the overall model was significant ($p = 0.001$). The corresponding proportions for fungi were 10.39% and 8.01%, and this overall model was also significant ($p = 0.001$).

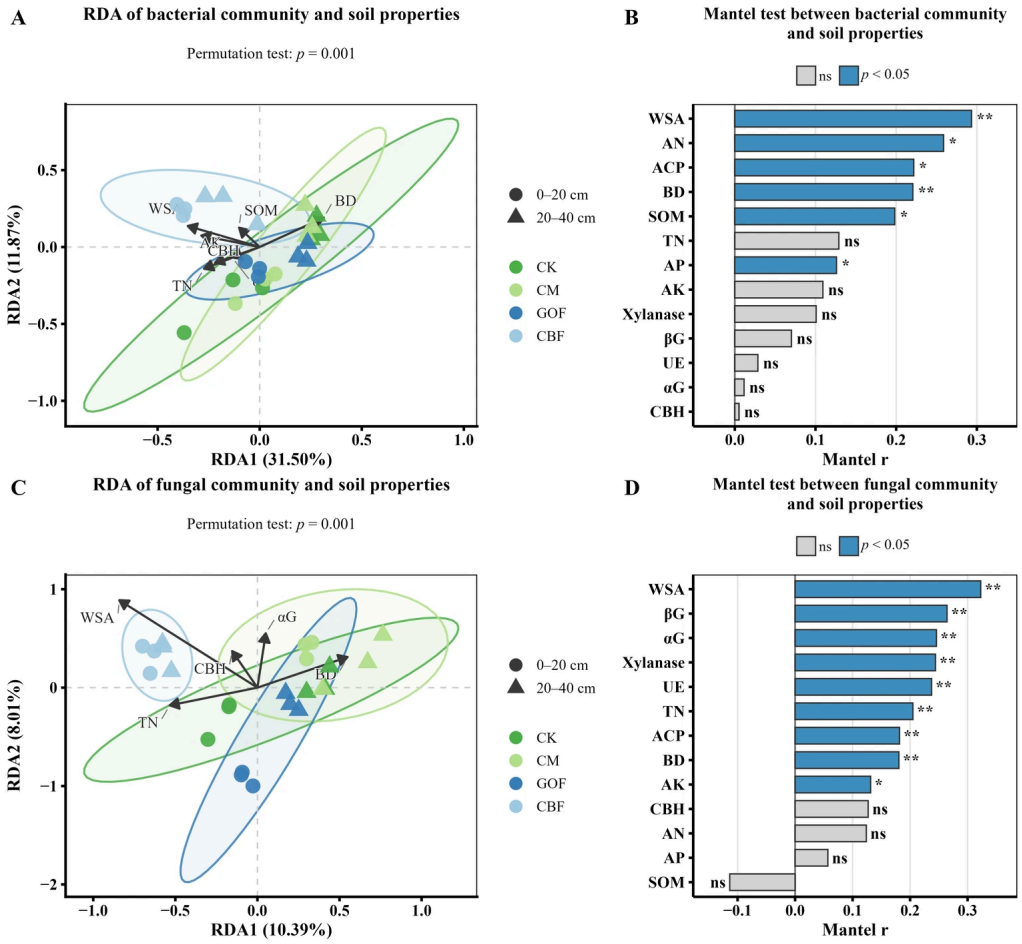


Figure 4. Relationships of soil properties and soil enzyme activities with bacterial and fungal community composition in 2025. Panels (**A**,**C**) show RDA of bacterial and fungal communities, respectively, and panels (**B**,**D**) show the corresponding Mantel tests. Colors indicate treatments and shapes indicate soil layers. In the Mantel plots, blue and gray bars indicate $p < 0.05$ and $p \geq 0.05$, respectively; *, **, and ns indicate $p < 0.05$, $p < 0.01$, and no significant association ($p \geq 0.05$), respectively.

According to the Mantel tests, bacterial community composition was significantly associated with WSA, AN, ACP, BD, SOM, and AP (Figure 4B). Fungal community composition was significantly associated with WSA, β-GC, α-GC, Xyl, UE, TN, ACP, BD, and AK (Figure 4D).

3.3.3. Bacterial–Fungal Cross-Kingdom Network and Network-Central Taxa

The bacterial–fungal cross-kingdom network contained 170 nodes and 545 edges. Bacteria represented 69.41% of the nodes and fungi 30.59%, while positive and negative associations represented 47.16% and 52.84% of the edges, respectively (Figure 5A). In the robustness analysis, betweenness-targeted node removal reduced network connectivity more rapidly than random removal (Figure 5B). After BH correction across all candidate pairs, 212 edges involving 113 nodes remained. Applying the same centrality criteria identified 11 network-central taxa, including 9 fungi and 2 bacteria. Of the 18 taxa identified in the original network, 17 remained connected in the FDR-filtered network, and 10 retained their network-central status (Table S2).

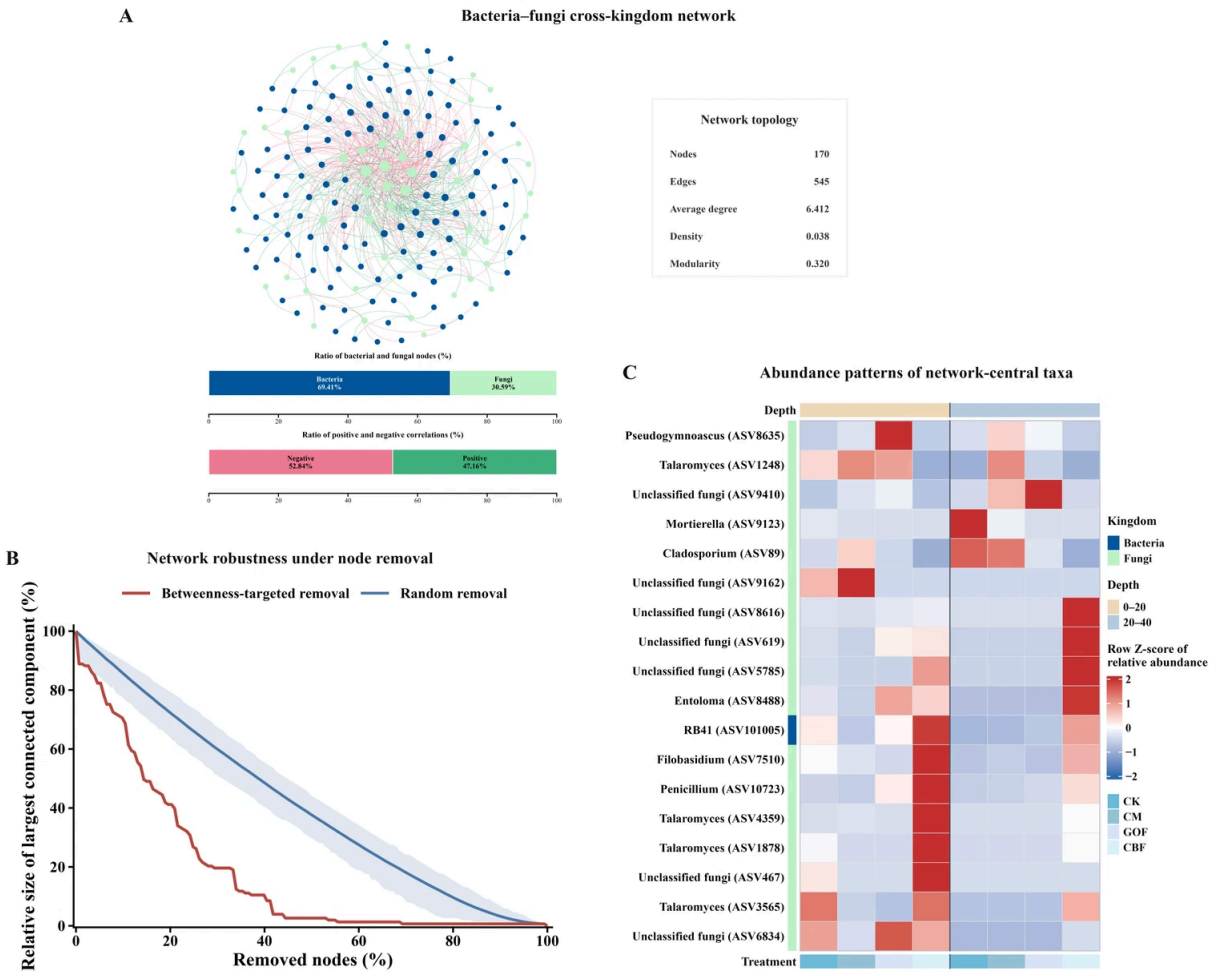


Figure 5. Bacterial–fungal cross-kingdom network, network robustness, and abundance of network-central taxa in 2025. (**A**) Cross-kingdom network constructed from 24 soil samples and its major topological properties. Blue and light-green nodes represent bacteria and fungi, respectively, whereas pink and green edges represent negative and positive associations. Bars below the network show the proportions of bacterial and fungal nodes and of positive and negative associations. (**B**) Network robustness under node removal. The random-removal curve represents the mean of 1000 simulations, with shading indicating the 95% confidence interval. Betweenness-targeted removal followed the fixed descending order of node betweenness calculated for the initial largest connected component, without recalculating betweenness after each removal. (**C**) Relative abundance of 18 network-central taxa across treatments and soil layers. Heatmap values are row-wise Z-scores of relative abundance; the top, bottom, and left color bars indicate soil layer, treatment, and microbial group, respectively. The network shown in panel A and the 18 taxa in panel C represent the original network based on unadjusted p values; FDR-filtered network results are provided in Table S2.

In the original network, 17 of the 18 network-central taxa were fungi and only one was a bacterium. Both Fisher's exact test and the randomization test indicated the significant enrichment of fungi among the network-central taxa (OR = 55.41, $p = 3.05 \times 10^{-9}$; randomization $p < 0.01$). Removing all network-central taxa reduced the largest connected component from 153 to 73 nodes, demonstrating a relative size of 0.477. This value was significantly lower than 0.831 obtained after the random removal of the same number of nodes ($p < 0.001$). The individual network-central taxa differed in relative abundance among treatments and soil layers (Figure 5C), although high relative abundances among these taxa were more common under CBF.

3.3.4. Microbial Community Cohesion and Soil Microbial Index

Bacterial community cohesion varied among organic amendment treatments (Figure 6A,B). In the 0–20 cm layer, CBF significantly increased bacterial positive cohesion by 6.07% relative to CK, whereas CM and GOF reduced it significantly by 7.64% and 10.09%, respectively. In the 20–40 cm layer, significant reductions in bacterial positive cohesion of 9.48%, 15.07%, and 14.11% occurred under CM, GOF, and CBF, respectively. Furthermore, significant treatment differences were observed for bacterial negative cohesion in both layers. Compared with CK in the 0–20 cm layer, CBF significantly reduced negative cohesion by 3.75%, whereas CM and GOF significantly increased it by 5.02% and 6.87%, respectively. In the 20–40 cm layer, the increases in bacterial negative cohesion of 7.12%, 7.38%, and 8.13% were identified under CM, GOF, and CBF, respectively, although the amendment treatments did not differ significantly from one another.

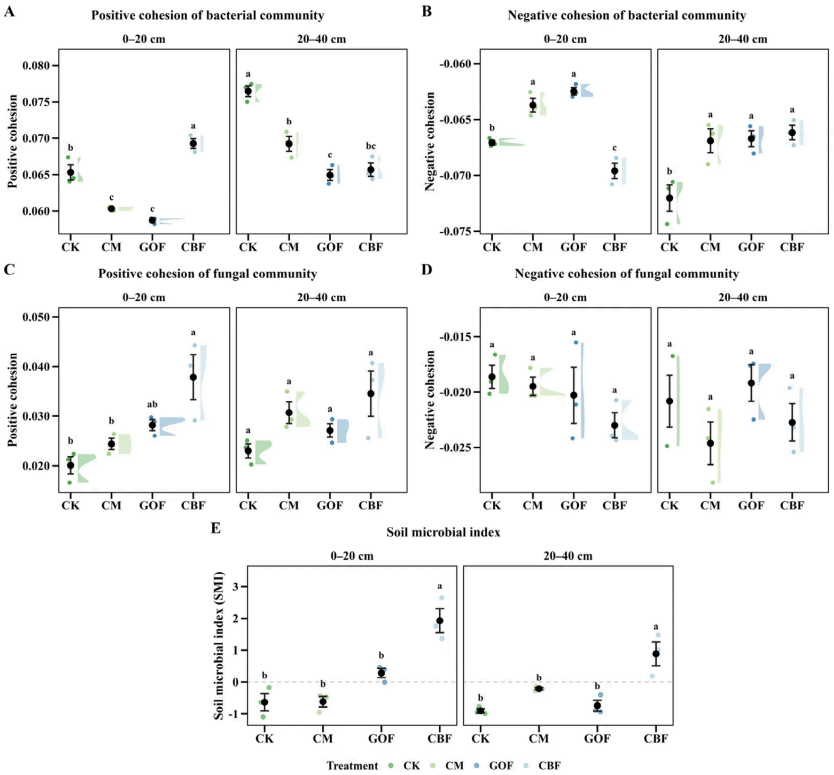


Figure 6. Bacterial and fungal community cohesion and soil microbial index (SMI) under different organic amendment treatments in 2025. (**A**,**B**) show bacterial positive and negative cohesion, respectively; (**C**,**D**) show fungal positive and negative cohesion, respectively; and (**E**) shows the soil microbial index (SMI). In (**A**–**D**), distribution shapes show data distributions, small points represent the three field replicates, and large points and error bars represent mean ± SE. In (**E**), small points represent field replicates, and large points and error bars represent mean ± SE. Colors indicate treatments. Different lowercase letters within the same soil layer indicate significant differences among treatments according to Tukey's test ($p < 0.05$).

For fungal community cohesion, a significant treatment effect was observed only for positive cohesion in the 0–20 cm layer (Figure 6C,D). In the 0–20 cm layer, CBF significantly increased fungal positive cohesion by 88.50% compared with CK, whereas no significant differences were observed among CK, CM, and GOF.

SMI integrated bacterial and fungal diversity, positive cohesion, and the relative abundance of network-central taxa and differed significantly among organic amendment treatments in both soil layers (Figure 6E). At 0–20 cm, SMI reached 1.93 under CBF and was significantly higher than that under every other treatment. The corresponding value at

20–40 cm was 0.89 and was significantly higher than that under the other treatments. Across the 12 alternative SMI formulations, CBF consistently showed the highest mean SMI in both soil layers (Table S3). However, the significance of pairwise differences depended partly on the weighting scheme. For example, the CBF–CM difference at 20–40 cm was significant under the original weighting scheme ($p = 0.0283$) but not under equal weighting ($p = 0.0645$).

3.4. Relationships Among Microorganisms, Soil Enzymes, and Soil Quality

SMI and SQI were significantly and positively correlated in the Spearman analysis ($\rho = 0.53$, $p < 0.01$; Figure 7A). For soil enzyme activities, SMI exhibited significant and positive correlations with both C_hydro and ACP, with a stronger relationship involving ACP ($\rho = 0.65$, $p < 0.001$). SQI was significantly and positively correlated with C_hydro and UE, and its relationship with C_hydro was stronger ($\rho = 0.84$, $p < 0.001$). Positive correlations of varying strengths were observed among C_hydro, UE, and ACP.

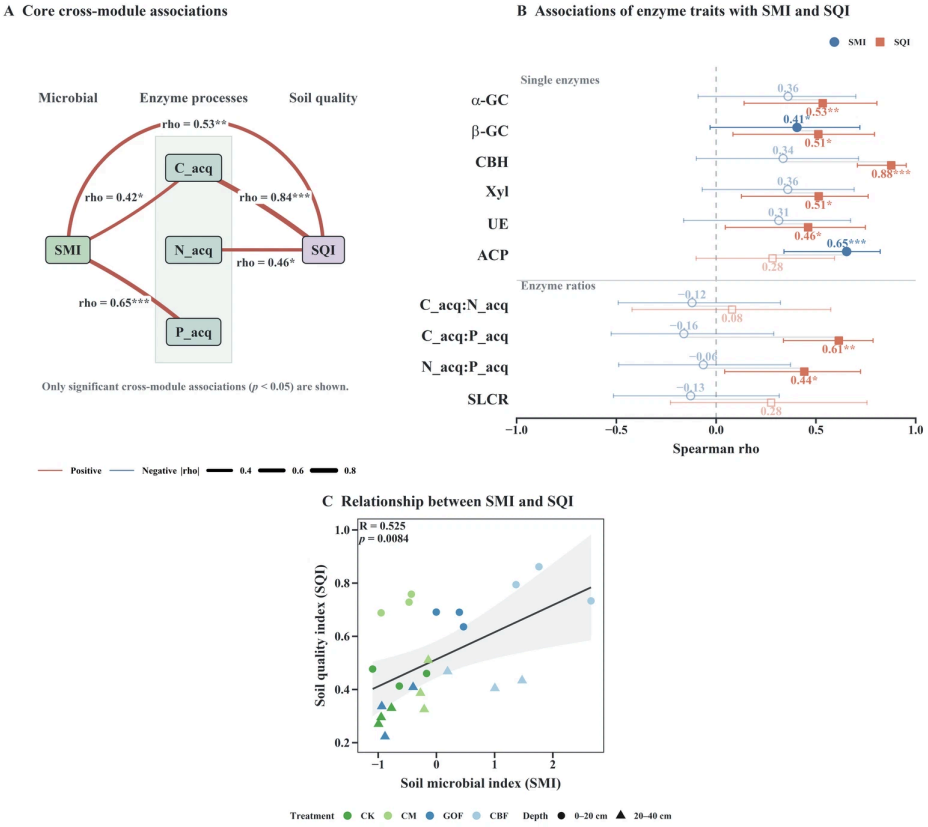


Figure 7. Relationships among the soil microbial index (SMI), soil enzyme activities, and soil quality index (SQI) in 2025. (**A**) Significant Spearman correlations among SMI, C_hydro, UE, ACP, and SQI; only cross-module correlations with $p < 0.05$ are shown. Red and blue lines indicate positive and negative correlations, respectively, and line width represents the absolute correlation coefficient ($|\rho|$). C_hydro represents the summed activities of α-GC, β-GC, CBH, and Xyl. (**B**) Spearman correlations of individual enzyme activities, C_hydro, and enzyme activity ratios with SMI and SQI. Blue circles and orange squares represent correlation coefficients with SMI and SQI, respectively, and horizontal lines indicate 95% confidence intervals. (**C**) Relationship between SMI and SQI. Colors indicate treatments, shapes indicate soil layers, and the solid line and shading represent the fitted relationship and its 95% confidence interval, respectively. *, **, and *** indicate $p < 0.05$, $p < 0.01$, and $p < 0.001$, respectively.

The associations between individual enzyme activities and SMI and SQI varied in strength among enzymes (Figure 7B). SMI was significantly and positively correlated with β-GC and ACP activities, most strongly with ACP ($\rho = 0.65$, $p < 0.001$). Significant positive correlations were observed between SQI and α-GC, β-GC, CBH, Xyl, and UE activities, with the strongest correlation observed with CBH ($\rho = 0.88$, $p < 0.001$). C_hydro was significantly and positively correlated with both SMI and SQI, whereas ACP was primarily related to SMI and UE primarily to SQI.

Although enzyme activity ratios presented weak correlations with SMI, C_hydro:ACP and UE:ACP were significantly and positively correlated with SQI (Figure 7B). C_hydro:UE and SLCR were not significantly correlated with either SMI or SQI. Thus, SMI, soil enzyme activities, and SQI were significantly associated, whereas the strengths of the relationships between individual activities or their ratios and the two indices varied.

3.5. Effects of Fertilization Treatments on Maize Grain Yield

Maize grain yield differed among fertilization treatments in both years (Figure 8). In 2024, grain yield under CM, GOF, and CBF was significantly higher than that under CK ($p < 0.05$), whereas no significant differences were observed among the three amendment treatments. A similar pattern was observed in 2025, with all three treatments producing significantly higher grain yields than CK ($p < 0.05$), while differences among CM, GOF, and CBF remained non-significant.

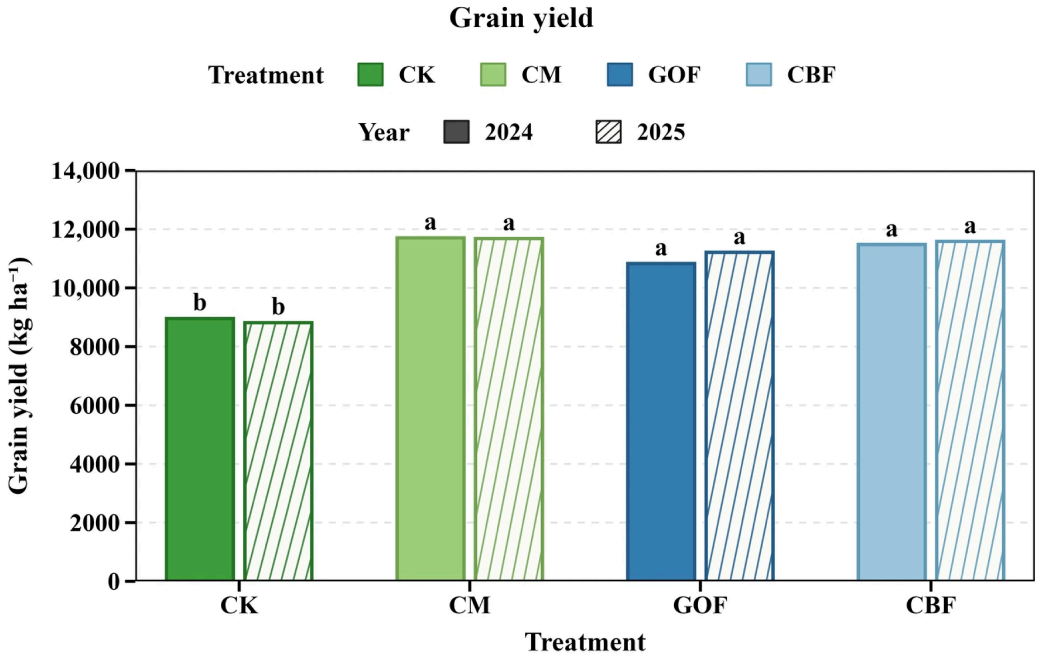


Figure 8. Effects of different fertilization treatments on maize grain yield in 2024 and 2025. Solid bars represent 2024, and hatched bars represent 2025. Different lowercase letters indicate significant differences among treatments within the same year ($p < 0.05$). Values represent the means of three field replicates (n = 3).

4. Discussion

4.1. Differences and Interannual Changes in the Soil Quality Improvement Effects of Organic Amendments

Under strip tillage with straw mulch retention, the three amendment-based fertilization strategies produced different soil responses, with their effects varying across years and soil depths [39]. The responses were more pronounced at 0–20 cm, with SQI being the highest

under CM in 2024 and under CBF in 2025. This indicates that the relative fertility-enhancing performance of the amendments shifted between the two consecutive years of application. The rapid accumulation of soil organic matter and nitrogen is the principal advantage of CM. Cattle manure contains abundant organic matter and organic nitrogen. After application, readily decomposable components are gradually mineralized by microorganisms, releasing mineral nitrogen. More recalcitrant components and their transformation products remain in the soil and increase its organic matter and nitrogen stocks [11]. The high SOM, TN, and AN under CM in 2024 and the persistence of the highest SOM in 2025 were consistent with continuous organic matter and nitrogen input [40]. Organic cementing agents and microbial metabolites can also promote soil-particle binding, thereby favoring the preservation of organic carbon within aggregates [10,39]. In contrast, CM did not consistently outperform the other treatments in terms of structural indicators, suggesting that organic matter accumulation and soil structural improvement may not necessarily occur in parallel. Amendment decomposition, soil depth, and initial soil structure may also influence structural responses.

The relative advantages of CBF over CM were more evident in the second year. Lower BD and higher AK primarily characterized CBF in 2024. By 2025, it combined the lowest surface BD with markedly higher WSA and relatively high AN, AP, and AK. However, this response was depth-dependent. In the 20–40 cm layer in 2025, BD under CBF was numerically higher than that under CK (1.581 vs. 1.512 g cm^{-3}), although the difference was not significant ($p > 0.05$). At the application rate of 1000 kg ha−1 and a carbon content of 8%, CBF supplied approximately 80 kg C ha−1 per application. This relatively small carbon input suggests that direct carbon incorporation alone may not fully explain the observed changes in soil structure. This pattern may be related to the low bulk density and porous nature of carbon components. After incorporation, this component may alter soil particle arrangement and pore conditions and facilitate aggregate formation [41,42]. As carbon components persist in the soil, their effects may accumulate over time. The absence of a CBF advantage in WSA in 2024 and its emergence in 2025 were consistent with a cumulative temporal response [43]. The carbon coating and controlled-release characteristics may also slow nutrient release [44]. These properties can reduce rapid nutrient release and loss over short periods and extend nutrient supply in soil [14,15]. Both the persistence of the carbon component and the nutrient-release process may be associated with CBF's second-year advantages in soil structure and the availability of some nutrients. Although GOF improved some soil properties, its overall effects at the application rate used in this experiment were less pronounced than those of CM and CBF.

Previous studies have also shown that the effects of organic amendments depend on input rates, amendment combinations, and soil management conditions. Laudicina et al. reported that compost input and tillage intensity jointly affected soil nutrient status and microbial biomass, highlighting the importance of both organic input and tillage management [45]. Lebrun et al. found that combining biochar with manure improved nutrient retention and microbial functional diversity, although the effects observed under field conditions were weaker than those in laboratory experiments [46]. Similarly, Paliaga et al. showed that treated wastewater irrigation increased soil total nitrogen and available phosphorus, while biochar and zeolite amendments helped alleviate salinity effects and increased microbial biomass carbon [47]. Although these studies differed from the present experiment in soil type, amendment composition, and experimental conditions, they indicate that the effects of organic amendments are influenced by nutrient inputs and the interactions between amendment materials and soil management. Therefore, the responses observed in this study should be interpreted as the effects of the overall fertilization strate-

gies under strip tillage with straw return, rather than being attributed solely to the intrinsic properties of individual amendment materials.

4.2. Changes in Soil Enzyme Activities and Microbial Communities and Their Relationships with Soil Properties

Soil enzyme activities demonstrated distinct amendment-dependent patterns. The significant increases in several C-related hydrolytic enzyme activities and UE activity under CM corresponded to higher SOM, TN, and AN. Cattle manure directly supplies organic carbon and nitrogen and provides microorganisms with abundant substrates for decomposition. Therefore, it may stimulate enzymes involved in organic carbon decomposition and nitrogen transformation [20,21]. Conversely, CBF exhibited higher ACP activity in both soil layers and the highest surface AP in 2025. Because CBF supplied the same nominal phosphorus input as CK, its higher AP could not be attributed to a greater phosphorus application rate. In Calciustolls, phosphate can be adsorbed onto soil mineral surfaces or retained through reactions with Ca, which may reduce phosphorus availability. The carbon coating and biochar component of CBF may alter these processes by affecting phosphorus adsorption and desorption, thereby influencing the retention and release of inorganic phosphorus. In addition, the higher ACP activity under CBF may promote the hydrolysis of organic phosphorus compounds, releasing inorganic phosphate and contributing to the available phosphorus pool. Therefore, the higher AP under CBF may be associated with both changes in inorganic phosphorus retention and mobilization and ACP-mediated organic phosphorus hydrolysis [48,49]. However, soil pH, carbonate content, phosphorus fractions, and phosphorus adsorption–desorption characteristics were not measured in this study. Thus, these processes provide plausible explanations for the observed changes in AP, but their individual contributions cannot be confirmed from the present measurements. The amendments also altered the relative relationships among the measured enzyme activities, with more pronounced changes at 20–40 cm. Across all three amendments, lower C_hydro:UE and SLCR but higher UE:ACP indicated marked relative shifts among enzyme activities involved in different nutrient transformations in the deeper soil layer.

Despite pronounced enzyme responses, most bacterial and fungal α-diversity indices changed little among treatments. Nevertheless, PCoA and PERMANOVA detected significant shifts in the composition of both communities [48,49]. Accordingly, short-term organic amendment application does not necessarily cause substantial changes in microbial richness or diversity. However, differences in amendment composition, nutrient supply, and soil structure may alter the relative abundances of microbial taxa [20–22,49]. Significant RDA and Mantel associations linked both bacterial and fungal communities to multiple soil structural, nutrient, and enzyme variables. Both communities were significantly correlated with WSA, while fungal communities were also closely related to several C-related hydrolytic enzyme activities, UE activity, and TN. These associations may arise because soil aggregates provide distinct microbial microenvironments and fungi participate in organic matter decomposition and nutrient transformation [10,39]. Fungi may also occupy important structural positions in bacterial–fungal association networks, as indicated by cross-kingdom networks. Fungi accounted for 17 of the 18 network-central taxa in the original network and 9 of the 11 central taxa in the FDR-filtered network. Removing central taxa or targeting high-betweenness nodes reduced network connectivity more than random removal. However, these simulations describe the topology of the inferred network rather than actual ecosystem stability. Because the network was constructed from 24 samples pooled across treatments and soil depths, shared environmental responses and within-plot dependence may have contributed to the observed associations. Therefore, these results do not establish direct ecological interactions or causal keystone functions.

4.3. Evaluation of the Soil Quality Improvement Effects of Organic Amendments Using SQI and SMI

The pooled correlations suggested positive associations among SMI, SQI, and several enzyme activities. Although a few associations remained nominally significant in the adjusted mixed-effects models, none remained significant after BH correction. This indicates that the pooled correlations may partly reflect shared responses to treatment and soil depth rather than independent relationships among microbial attributes, enzyme activities, and soil quality. Therefore, these correlations should be interpreted as exploratory associations rather than evidence of direct functional or causal relationships.

Collectively, the physicochemical, enzyme, and microbial results suggested that the amendments may contribute to the improvement of Calciustoll fertility through distinct processes. For CM, higher inputs of organic matter and nitrogen were accompanied by higher C-related hydrolytic enzyme activities and UE activity, ultimately resulting in pronounced SOM and nitrogen accumulation [11,20,21]. In contrast, CBF presented a different pattern in the second year, with lower BD, higher WSA, greater availability of some nutrients, and a higher SMI. The persistence of the carbon component, nutrient release from the coated granules, and the resulting changes in the soil environment may all be associated with these responses [14,15,42]. At the application rate used in this experiment, GOF improved some soil properties but had relatively small overall effects. Treatment-induced changes in soil enzyme activities and microbial communities were associated with changes in nutrient availability and soil structure, and these integrated responses were ultimately reflected in differences in SQI.

Under the examined field conditions, changes in soil enzyme activities and microbial communities were accompanied by improvements in nutrient availability and soil structure. Together, these responses were reflected in higher overall soil quality. Organic matter and nitrogen accumulation were more prominent under CM, whereas CBF showed broader improvements in soil structure, nutrients, SMI, and SQI during the second consecutive year of application. These findings provide field-based evidence for selecting amendment treatments in semiarid Calciustoll systems under comparable management conditions, although their longer-term effects and transferability require further evaluation.

5. Conclusions

All three organic amendments improved Calciustoll fertility to varying degrees under strip tillage with straw mulch retention; however, the nature of these gains differed. CM primarily promoted soil organic matter and nitrogen accumulation, accompanied by increased C-related hydrolytic enzyme activities and UE activity. CBF produced more pronounced improvements in soil structure and the availability of several nutrients in the second year. Most bacterial and fungal α-diversity indices changed little, but the amendments significantly altered community composition, which was closely associated with soil structure, nutrient availability, and enzyme activities. The relationships among SMI, SQI, and enzyme activities were exploratory and were not maintained after accounting for treatment, soil depth, and plot-level structure. Under these application conditions, CM more strongly promoted organic matter and nitrogen accumulation, whereas CBF produced broader improvements in soil structure, nutrient availability, SQI, and SMI in the second consecutive year of application. GOF also improved soil fertility, but its overall effects were weaker.

Supplementary Materials: The following supporting information can be downloaded at https://www.mdpi.com/article/10.3390/agronomy16222326/s1. Table S1. Annual carbon and nutrient inputs under different fertilization treatments. Table S2. Sensitivity analysis of the bacterial–fungal

cross-kingdom network. Table S3. Sensitivity analysis of the soil microbial index (SMI) under alternative weighting schemes and indicator combinations. Table S4. Assay conditions and unit conversion procedures for soil enzyme activities. Table S5. Pooled and experimental-structure-adjusted results for all 26 unique association tests. Figure S1. Original and FDR-corrected bacterial–fungal association networks. Table S6. Restricted PERMDISP diagnostics for bacterial and fungal communities. Figure S2. Soil classification profile.

Author Contributions: Z.B.: Writing, Conceptualization, Data curation, Software, Visualization, Methodology. C.G.: Writing. Y.H.: Writing. B.C.: Resources, Formal analysis. J.L.: Validation, Supervision. Y.S.: Project administration. J.C.: Investigation. Y.Y.: Software. C.Z.: Validation. H.W.: Funding acquisition, Supervision, Writing—review and editing. B.S.: Conceptualization, Formal analysis, Project administration. All authors have read and agreed to the published version of the manuscript.

Funding: This work was supported by the National Key R&D Program of China (Grant No. 2023YFD1501105), the Jilin Province Science and Technology Development Plan (Grant No. 20240203007NC), and the Graduate Student Fund of Jilin Agricultural Science and Technology Innovation Project (Grant No. E60010536).

Data Availability Statement: The original data presented in the study are openly available in the NCBI database at BioProject PRJNA1537959.

Conflicts of Interest: The authors declare no conflicts of interest.

References

1. Deserts, Semiarid Areas and Desertification. In *Climate Change 2022—Impacts, Adaptation and Vulnerability*; Cambridge University Press: Cambridge, UK, 2023; pp. 2195–2232.
2. Labaz, B.; Hartemink, A.E.; Zhang, Y.; Stevenson, A.; Kabała, C. Organic Carbon in Mollisols of the World—A Review. *Geoderma* **2024**, *447*, 116937. [CrossRef]
3. Yuan, J.; Liu, J.; Cheng, S.; Zhang, S.; Zhang, H.; Liu, S.; Ren, J.; Liang, Y.; Cai, H. Differences of Physicochemical Properties of Black and Light Chernozem Soils in 0–100 Cm Soil Layer with Different Yield Levels under Long-Term Maize Cropping System. *J. Plant Nutr. Fertil.* **2021**, *27*, 802–813. [CrossRef]
4. Cong, P.; Yin, G.; Gu, J. Effects of Stubble and Mulching on Soil Erosion by Wind in Semi-Arid China. *Sci. Rep.* **2016**, *6*, 29966. [CrossRef] [PubMed]
5. Qin, X.; Huang, T.; Lu, C.; Dang, P.; Zhang, M.; Guan, X.; Wen, P.; Wang, T.-C.; Chen, Y.; Siddique, K.H.M. Benefits and Limitations of Straw Mulching and Incorporation on Maize Yield, Water Use Efficiency, and Nitrogen Use Efficiency. *Agric. Water Manag.* **2021**, *256*, 107128. [CrossRef]
6. Xin, J.; Yan, L.; Cai, H. Response of Soil Organic Carbon to Straw Return in Farmland Soil in China: A Meta-Analysis. *J. Environ. Manag.* **2024**, *359*, 121051. [CrossRef] [PubMed]
7. Jabro, J.D.; Stevens, W.B.; Iversen, W.M.; Evans, R.G. Technical Note: Bulk Density, Water Content, and Hydraulic Properties of a Sandy Loam Soil Following Conventional or Strip Tillage. *Appl. Eng. Agric.* **2011**, *27*, 765–768. [CrossRef]
8. Ren, L.; Nest, T.V.; Ruysschaert, G.; D'Hose, T.; Cornelis, W.M. Short-Term Effects of Cover Crops and Tillage Methods on Soil Physical Properties and Maize Growth in a Sandy Loam Soil. *Soil Tillage Res.* **2019**, *192*, 76–86. [CrossRef]
9. Wang, C.; Ai, S.; Chen, Q.; Li, J.; Ding, J.; Yang, F. Effect of Strip Tillage Widths on Soil Moisture, Soil Temperature and Soil Structure in Northeast China. *Front. Environ. Sci.* **2024**, *12*, 1404971. [CrossRef]
10. Ma, S.; Cao, Y.; Lu, J.; Ren, T.; Cong, R.; Lu, Z.; Zhu, J.; Li, X. Response of Soil Aggregation and Associated Organic Carbon to Organic Amendment and Its Controls: A Global Meta-Analysis. *CATENA* **2024**, *237*, 107774. [CrossRef]
11. Gross, A.; Glaser, B. Meta-Analysis on How Manure Application Changes Soil Organic Carbon Storage. *Sci. Rep.* **2021**, *11*, 5516. [CrossRef] [PubMed]
12. Zhai, L.; Zheng, M.; Zhang, L.; Chen, J.; Zhang, J.; Jia, X. Short-Term Co-Application of Organic and Chemical Fertilizer Benefits Topsoil Properties and Maize Productivity in a Medium-Productivity Meadow-Cinnamon Soil. *Agronomy* **2023**, *13*, 944. [CrossRef]
13. Niedziński, T.; Sierra, M.J.; Łabętowicz, J.; Noras, K.; Cabrales, C.; Millán, R. Release of Nitrogen from Granulate Mineral and Organic Fertilizers and Its Effect on Selected Chemical Parameters of Soil. *Agronomy* **2021**, *11*, 1981. [CrossRef]
14. Vejan, P.; Khadiran, T.; Abdullah, R.; Ahmad, N. Controlled Release Fertilizer: A Review on Developments, Applications and Potential in Agriculture. *J. Control. Release* **2021**, *339*, 321–334. [CrossRef] [PubMed]
15. Mansouri, H.; Ait Said, H.; Noukrati, H.; Oukarroum, A.; Ben youcef, H.; Perreault, F. Advances in Controlled Release Fertilizers: Cost-Effective Coating Techniques and Smart Stimuli-Responsive Hydrogels. *Adv. Sustain. Syst.* **2023**, *7*, 2300149. [CrossRef]

16. Shofiati, S.; Nugroho, G.A.; Kusuma, Z.; Kurniawan, S. Effect of Biochar-Coated Urea on Soil Nitrogen, Plant Uptake, and Sweet Corn Yield in Sandy Soil. *Nitrogen* **2025**, *6*, 61. [CrossRef]
17. Wang, C.; Luo, D.; Zhang, X.; Huang, R.; Cao, Y.; Liu, G.; Zhang, Y.; Wang, H. Biochar-Based Slow-Release of Fertilizers for Sustainable Agriculture: A Mini Review. *Environ. Sci. Ecotechnol.* **2022**, *10*, 100167. [CrossRef] [PubMed]
18. Cui, Y.; Moorhead, D.L.; Peng, S.; Sinsabaugh, R.L. New Insights into the Patterns of Ecoenzymatic Stoichiometry in Soil and Sediment. *Soil Biol. Biochem.* **2023**, *177*, 108910. [CrossRef]
19. Moorhead, D.; Cui, Y.; Sinsabaugh, R.; Schimel, J. Interpreting Patterns of Ecoenzymatic Stoichiometry. *Soil Biol. Biochem.* **2023**, *180*, 108997. [CrossRef]
20. Liu, W.; Yang, Z.; Ye, Q.; Peng, Z.; Zhu, S.; Chen, H.; Liu, D.; Li, Y.; Deng, L.; Shu, X.; et al. Positive Effects of Organic Amendments on Soil Microbes and Their Functionality in Agro-Ecosystems. *Plants* **2023**, *12*, 3790. [CrossRef] [PubMed]
21. Liu, X.; Liu, H.; Zhang, Y.; Liu, C.; Liu, Y.; Li, Z.; Zhang, M. Organic Amendments Alter Microbiota Assembly to Stimulate Soil Metabolism for Improving Soil Quality in Wheat–Maize Rotation System. *J. Environ. Manag.* **2023**, *339*, 117927. [CrossRef] [PubMed]
22. Tang, S.; Ma, Q.; Marsden, K.A.; Chadwick, D.R.; Luo, Y.; Kuzyakov, Y.; Wu, L.; Jones, D.L. Microbial Community Succession in Soil Is Mainly Driven by Carbon and Nitrogen Contents Rather than Phosphorus and Sulphur Contents. *Soil Biol. Biochem.* **2023**, *180*, 109019. [CrossRef]
23. Lehmann, J.; Bossio, D.A.; Kögel-Knabner, I.; Rillig, M.C. The Concept and Future Prospects of Soil Health. *Nat. Rev. Earth Env.* **2020**, *1*, 544–553. [CrossRef] [PubMed]
24. Andrews, S.S.; Karlen, D.L.; Mitchell, J.P. A Comparison of Soil Quality Indexing Methods for Vegetable Production Systems in Northern California. *Agric. Ecosyst. Environ.* **2002**, *90*, 25–45. [CrossRef]
25. Yoder, R.E. A Direct Method of Aggregate Analysis of Soils and a Study of the Physical Nature of Erosion Losses. *Agron. J.* **1936**, *28*, 337–351. [CrossRef]
26. Callahan, B.J.; McMurdie, P.J.; Rosen, M.J.; Han, A.W.; Johnson, A.J.A.; Holmes, S.P. DADA2: High-Resolution Sample Inference from Illumina Amplicon Data. *Nat. Methods* **2016**, *13*, 581–583. [CrossRef] [PubMed]
27. Bolyen, E.; Rideout, J.R.; Dillon, M.R.; Bokulich, N.A.; Abnet, C.C.; Al-Ghalith, G.A.; Alexander, H.; Alm, E.J.; Arumugam, M.; Asnicar, F.; et al. Reproducible, Interactive, Scalable and Extensible Microbiome Data Science Using QIIME 2. *Nat. Biotechnol.* **2019**, *37*, 852–857. [CrossRef] [PubMed]
28. Kõljalg, U.; Nilsson, R.H.; Abarenkov, K.; Tedersoo, L.; Taylor, A.F.S.; Bahram, M.; Bates, S.T.; Bruns, T.D.; Bengtsson-Palme, J.; Callaghan, T.M.; et al. Towards a Unified Paradigm for Sequence-Based Identification of Fungi. *Mol. Ecol.* **2013**, *22*, 5271–5277. [CrossRef] [PubMed]
29. Quast, C.; Pruesse, E.; Yilmaz, P.; Gerken, J.; Schweer, T.; Yarza, P.; Peplies, J.; Glöckner, F.O. The SILVA Ribosomal RNA Gene Database Project: Improved Data Processing and Web-Based Tools. *Nucleic Acids Res.* **2013**, *41*, D590–D596. [CrossRef] [PubMed]
30. Anderson, M.J. A New Method for Non-Parametric Multivariate Analysis of Variance. *Austral Ecol.* **2001**, *26*, 32–46. [CrossRef]
31. Legendre, P.; Gallagher, E.D. Ecologically Meaningful Transformations for Ordination of Species Data. *Oecologia* **2001**, *129*, 271–280. [CrossRef] [PubMed]
32. Barberán, A.; Bates, S.T.; Casamayor, E.O.; Fierer, N. Using Network Analysis to Explore Co-Occurrence Patterns in Soil Microbial Communities. *ISME J.* **2012**, *6*, 343–351. [CrossRef] [PubMed]
33. Chen, L.; Dini-Andreote, F.; Liu, H.; Wang, H.; Dumbrell, A.; Wang, Z.; Chen, X.; Chen, F.; Chen, X.; Wu, L.; et al. Integrating Variation in Bacterial–Fungal Co-Occurrence Network with Soil Carbon Dynamics. *J. Appl. Ecol.* **2024**, *61*, 36–50. [CrossRef]
34. Amit, G.; Bashan, A. Top-down Identification of Keystone Taxa in the Microbiome. *Nat. Commun.* **2023**, *14*, 3951. [CrossRef] [PubMed]
35. Miklós, I.; Podani, J. Randomization of Presence–Absence Matrices: Comments and New Algorithms. *Ecology* **2004**, *85*, 86–92. [CrossRef]
36. Friedman, J.; Alm, E.J. Inferring Correlation Networks from Genomic Survey Data. *PLoS Comput. Biol.* **2012**, *8*, e1002687. [CrossRef] [PubMed]
37. Herren, C.M.; McMahon, K.D. Cohesion: A Method for Quantifying the Connectivity of Microbial Communities. *ISME J.* **2017**, *11*, 2426–2438. [CrossRef] [PubMed]
38. Tukey, J.W. Comparing Individual Means in the Analysis of Variance. *Biometrics* **1949**, *5*, 99. [CrossRef]
39. Or, D.; Keller, T.; Schlesinger, W.H. Natural and Managed Soil Structure: On the Fragile Scaffolding for Soil Functioning. *Soil Tillage Res.* **2021**, *208*, 104912. [CrossRef]
40. Ren, J.; Liu, X.; Yang, W.; Yang, X.; Li, W.; Xia, Q.; Li, J.; Gao, Z.; Yang, Z. Rhizosphere Soil Properties, Microbial Community, and Enzyme Activities: Short-Term Responses to Partial Substitution of Chemical Fertilizer with Organic Manure. *J. Environ. Manag.* **2021**, *299*, 113650. [CrossRef] [PubMed]
41. Islam, M.U.; Jiang, F.; Guo, Z.; Peng, X. Does Biochar Application Improve Soil Aggregation? A Meta-Analysis. *Soil Tillage Res.* **2021**, *209*, 104926. [CrossRef]

42. Singh, H.; Northup, B.K.; Rice, C.W.; Prasad, P.V.V. Biochar Applications Influence Soil Physical and Chemical Properties, Microbial Diversity, and Crop Productivity: A Meta-Analysis. *Biochar* **2022**, *4*, 8. [CrossRef]
43. Ma, N.; Zhang, L.; Zhang, Y.; Yang, L.; Yu, C.; Yin, G.; Doane, T.A.; Wu, Z.; Zhu, P.; Ma, X. Biochar Improves Soil Aggregate Stability and Water Availability in a Mollisol after Three Years of Field Application. *PLoS ONE* **2016**, *11*, e0154091. [CrossRef] [PubMed]
44. Costa, J.D.L.; Lustosa Filho, J.F.; Viana, R.D.S.R.; Chagas, J.K.M.; Figueiredo, C.C.D. Nutrient Release, Leaching, and Agronomic Performance of Additive-Enhanced Biochar-Based Fertilizers: A Global Meta-Analysis. *Agriculture* **2026**, *16*, 1147. [CrossRef]
45. Laudicina, V.A.; Badalucco, L.; Palazzolo, E. Effects of Compost Input and Tillage Intensity on Soil Microbial Biomass and Activity under Mediterranean Conditions. *Biol. Fertil. Soils* **2011**, *47*, 63–70. [CrossRef]
46. Lebrun, M.; Zahid, Z.; Bednik, M.; Medynska-Juraszek, A.; Száková, J.; Brtnický, M.; Holátko, J.; Bourgerie, S.; Beesley, L.; Pohořelý, M.; et al. Combined Biochar and Manure Addition to an Agricultural Soil Benefits Fertility, Microbial Activity, and Mitigates Manure-induced CO_2 Emissions. *Soil Use Manag.* **2024**, *40*, e12997. [CrossRef]
47. Paliaga, S.; Muscarella, S.M.; Alduina, R.; Badalucco, L.; Bulacio Fischer, P.T.; Di Leto, Y.; Gallo, G.; Mannina, G.; Laudicina, V.A. The Effects of Enriched Biochar and Zeolite and Treated Wastewater Irrigation on Soil Fertility and Tomato Growth. *J. Environ. Manag.* **2025**, *380*, 124990. [CrossRef] [PubMed]
48. Sun, C.; Yang, X.; Wen, Z.; Lian, Y. Effects of Partial Organic Fertilizer Substitution on Soil Physicochemical Properties, Enzyme Activities, Microbial Communities, and Maize Yield: A Two-Year Field Study. *Agronomy* **2026**, *16*, 1296. [CrossRef]
49. Zhang, S.; Li, X.; Chen, K.; Shi, J.; Wang, Y.; Luo, P.; Yang, J.; Wang, Y.; Han, X. Long-Term Fertilization Altered Microbial Community Structure in an Aeolian Sandy Soil in Northeast China. *Front. Microbiol.* **2022**, *13*, 979759. [CrossRef] [PubMed]

Disclaimer/Publisher's Note: The statements, opinions and data contained in all publications are solely those of the individual author(s) and contributor(s) and not of MDPI and/or the editor(s). MDPI and/or the editor(s) disclaim responsibility for any injury to people or property resulting from any ideas, methods, instructions or products referred to in the content.